jove

Utilizing Time-Resolved Protein-Induced Fluorescence Enhancement to Identify Stable Local Conformations One α-Synuclein Monomer at a Time

Sofia Zaer[1], **Eitan Lerner**[1,2]

[1] Department of Biological Chemistry, The Alexander Silberman Institute of Life Sciences, Faculty of Mathematics & Science, The Edmond J. Safra Campus, The Hebrew University of Jerusalem [2] The Center for Nanoscience and Nanotechnology, The Hebrew University of Jerusalem

Corresponding Author

Eitan Lerner
eitan.lerner@mail.huji.ac.il

Citation

Zaer, S., Lerner, E. Utilizing Time-Resolved Protein-Induced Fluorescence Enhancement to Identify Stable Local Conformations One α-Synuclein Monomer at a Time. *J. Vis. Exp.* (171), e62655, doi:10.3791/62655 (2021).

Date Published

May 30, 2021

DOI

10.3791/62655

URL

jove.com/video/62655

Abstract

Using spectroscopic rulers to track multiple conformations of single biomolecules and their dynamics have revolutionized the understanding of structural dynamics and its contributions to biology. While the FRET-based ruler reports on inter-dye distances in the 3-10 nm range, other spectroscopic techniques, such as protein-induced fluorescence enhancement (PIFE), report on the proximity between a dye and a protein surface in the shorter 0-3 nm range. Regardless of the method of choice, its use in measuring freely-diffusing biomolecules one at a time retrieves histograms of the experimental parameter yielding separate centrally-distributed sub-populations of biomolecules, where each sub-population represents either a single conformation that stayed unchanged within milliseconds, or multiple conformations that interconvert much faster than milliseconds, and hence an averaged-out sub-population. In single-molecule FRET, where the reported parameter in histograms is the inter-dye FRET efficiency, an intrinsically disordered protein, such as the α-Synuclein monomer in buffer, was previously reported as exhibiting a single averaged-out sub-population of multiple conformations interconverting rapidly. While these past findings depend on the 3-10 nm range of the FRET-based ruler, we sought to put this protein to the test using single-molecule PIFE, where we track the fluorescence lifetime of site-specific sCy3-labeled α-Synuclein proteins one at a time. Interestingly, using this shorter range spectroscopic proximity sensor, sCy3-labeled α-Synuclein exhibits several lifetime sub-populations with distinctly different mean lifetimes that interconvert in 10-100 ms. These results show that while α-Synuclein might be disordered globally, it nonetheless attains stable local structures. In summary, in this work we highlight the advantage of using different spectroscopic proximity sensors that track local or global structural changes one biomolecule at a time.

Introduction

Over the past two decades, single-molecule fluorescence-based methods have become a powerful tool for measuring biomolecules[1,2], probing how different biomolecular parameters distribute as well as how they dynamically interconvert between different sub-populations of these parameters at sub-millisecond resolution[3,4,5]. The parameters in these techniques include the energy transfer efficiency in FRET measurements [6,7], fluorescence anisotropy[8,9], fluorescence quantum yields and lifetimes[10,11], as a function of different fluorescence quenching[12] or enhancement[13] mechanisms. One of these mechanisms, better known as protein-induced fluorescence enhancement (PIFE)[14] introduces the enhancement of fluorescence quantum yield and lifetime as a function of steric obstruction to the free isomerization of the fluorophore when in excited-state, caused by protein surfaces in the vicinity of the dye[14,15,16,17,18,19]. Both FRET and PIFE are considered spectroscopic rulers or proximity sensors since their measured parameter is directly linked to a spatial measure within the labeled biomolecule under measurement. While the FRET efficiency is related to the distance between a pair of dyes within a range of 3-10 nm[20], PIFE tracks increases in fluorescence quantum yields or lifetimes related to the distance between the dye and a surface of a nearby protein in the range of 0-3 nm[19].

Single-molecule FRET has been widely used for providing structural insights into many different protein systems, including intrinsically disordered proteins (IDPs)[21], such as α-Synuclein (α-Syn)[22]. α-Syn can form ordered structures following binding to different biomolecules and under different conditions[23,24,25,26,27,28,29,30]. However, when unbound, the α-Syn monomer is characterized by high conformational heterogeneity with rapidly interconverting conformations[31,32].

The conformations of α-Syn have been studied previously using various different techniques that help in identifying conformational dynamics of such highly heterogeneous and dynamic protein systems[33,34,35,36,37,38,39]. Interestingly, single-molecule FRET (smFRET) measurements of α-Syn in buffer reported a single FRET population[39,40] that is an outcome of time-averaging of conformations dynamically interconverting at times much faster than the typical diffusion time of α-Syn through the confocal spot (times as fast as few microseconds and even faster than that, relative to typical millisecond diffusion times)[40,41]. However, using a FRET spectroscopic ruler with the 3-10 nm distance sensitivity sometimes reports only on overall structural changes in a small protein such as α-Syn. Single-molecule measurements utilizing spectroscopic proximity sensors with shorter distance sensitivities have the potential to report on dynamics of local structures. Herein we perform single-molecule PIFE measurements of α-Syn and identify different sub-populations of fluorescence lifetimes mapping to different local structures with transitions between them as slow as 100 ms. This work summarizes time-resolved smPIFE measurements of freely-diffusing α-Syn molecules one at a time, in buffer and when bound to SDS-based membranes as a short-range single-molecule spectroscopic proximity sensor.

Protocol

1. Plasmid transformation

1. Preparation of 0.5 L of SOC medium

1. Weigh 10 g of tryptone, 2.5 g of Yeast extract, 0.25 g of sodium chloride (NaCl), 0.1 g of potassium chloride (KCl).
2. Add double-distilled water (DDW) until total volume of 0.5 L.
3. Adjust to pH 7 by adding sodium hydroxide (NaOH).
4. Prepare stock aliquots of 100 mL and autoclave.
5. Before using, add 0.5 mL of sterile magnesium chloride ($MgCl_2$) and 1.8 mL of sterile glucose to 100 mL of SOC.

2. Thaw BL21 (DE3) competent *Escherichia coli* cells on ice.
3. Mix the competent cells gently.
4. Prepare two 15 mL tubes. Label one as transformation reaction tube and the other one as the control tube.
5. Aliquot 100 µL of competent cells into the tubes.
6. Add 1 µL of plasmid at a concentration of 0.1 ng/µL into the transformation reaction tube.
7. Heat SOC medium in 42 °C water bath for use in step 1.8.
8. Heat-pulse the two tubes in 42 °C water bath for a duration of **45 seconds**. (Critical step!)
9. Add 900 µL of heated SOC medium to each tube.
10. Incubate the tubes at 37 °C for a duration of 45 minutes with shaking at a velocity of 225 rpm.
11. Spread 200 µL of the cells with the transformed plasmid onto one LB (Luria-Bertani)-agar plate containing 100 µg/mL ampicillin, using a sterile cell spreader.
12. Spread 200 µL of the cells with the transformed plasmid onto one LB-agar plate without ampicillin, using a sterile spreader **(positive control)**.
13. Spread 200 µL of the control cells (not containing a plasmid) onto one LB-agar plate containing 100 µg/mL ampicillin, using a sterile spreader (**negative control**).
14. Incubate the plates overnight at 37 °C.

2. Protein preparation

1. Recombinant α-Synuclein expression and purification
    1. Pick a single colony and grow in 100 mL of autoclaved LB (Luria-Bertani) liquid medium containing 100 µg/mL ampicillin at 37 °C **(starter)**.
    2. Prepare four 2 L Erlenmeyer flasks, each containing 1 L of autoclaved LB medium and 100 µg/mL ampicillin **(large inoculation)**.
    3. Measure the optical density (OD at λ = 600 nm) of the cell solution. When the cell density of the starter reaches an $OD_{\lambda=600nm}$ of 0.6-0.7, add 10 mL of starter solution per each 1 L of LB medium prepared in the previous step.
    4. Grow the bacterial mediums in an incubator shaker at 37 °C and a velocity of 200 rpm.
    5. When the cell density reaches an $OD_{\lambda=600nm}$ of 0.6-0.8, induce protein expression by adding isopropyl β-d-1-thiogalactopyranoside (IPTG) per each 1 L of growth medium to a final concentration of 1 mM.
    NOTE: Dissolve 0.96 g of IPTG in 4 mL of DDW and add 1 mL of the resulting IPTG solution per each 1 L of bacterial growth.
    6. Grow the cells for a duration of 4 hours and collect them by centrifugation in 50 mL tubes at a velocity of 5,170 x g for a duration of 8 minutes.

NOTE: In each round, discard the supernatant, keep the pellet and fill again the same tubes with bacterial growth.

7. Store the bacterial pellet in deep freeze storage (e.g., -80 °C) for the next day.
8. The next day, prepare 200 mL of lysis buffer: 40% (w/v) sucrose and buffer A, which includes 30 mM Tris-HCl, 2 mM ethylenediaminetetraacetic acid (EDTA), 2 mM dithiothreitol (DTT) at pH 8.0.
9. Add 25 mL of lysis buffer to each tube with bacterial pellet.
10. Re-suspend the pellet (use sterile plastic Pasteur pipettes) in Lysis buffer (see 2.1.8).
11. Prepare sterile 250 mL Erlenmeyer flask with a stirrer magnet on ice.
12. Add 5 mL of lysis buffer, and then transfer the homogeneous re-suspended cells to it.
13. Stir the cells for a duration of 20 minutes at 200 rpm at room temperature.
14. Divide the solution into 50 mL tubes and centrifuge at 4 °C for a duration of 30 minutes at a velocity of 17,400 x g.
15. Discard the supernatant.
16. Prepare sterile 250 mL Erlenmeyer flask with stirrer magnet on ice.
17. Add 15 mL of dissolution buffer (90 mL cooled buffer A and 37 µL of $MgCl_2$ dissolved beyond the solubility limit and filtered) into each tube. Use sterile plastic Pasteur pipettes and dissolve the pellet.
18. When part of the solution becomes homogeneous, move it to a stirred Erlenmeyer flask on ice.
19. Determine the solution volume in the Erlenmeyer.
20. Add 10 mg of streptomycin sulfate per each 1 mL of solution (before adding, dissolve streptomycin sulfate in 2 mL of buffer A).
    NOTE: This step is performed in order to remove the DNA and ribosomes away.
21. Stir the solution for a duration of 10-20 minutes at room temperature.
22. Divide the solution into 50 mL tubes and centrifuge at 4 °C and at a velocity of 20,700 x g for a duration of 30 minutes.
23. Collect the supernatant and discard the pellet.
24. Prepare a sterile 250 mL Erlenmeyer flask on ice with a stirrer.
25. Filter the supernatant using 0.22 µm syringe filter into the clean Erlenmeyer flask.
26. Determine the solution volume and weigh 0.3 g of ammonium sulfate per each 1 mL of solution.
27. Gradually, add the ammonium sulfate to the stirred solution.
    NOTE: This step is performed to precipitate proteins. When the ammonium sulfate binds the proteins, the solution becomes obscured and blurry, which shows up as white color.
28. Stir for 30 minutes at room temperature.
29. Divide the solution to 50 mL tubes and centrifuge at 4 °C and at a velocity of 20,700 g for a duration of 30 minutes.
30. Carefully discard the supernatant and keep the pellet.
31. Dissolve the pellet with 20 mL of Buffer A.

32. Unify all the solutions into one tube, and then measure the UV absorption spectrum of the solution.
NOTE: If the spectrum shows a signature of aggregation (absorption above a wavelength of 300 nm), continue to the next step. If not, skip the next step and move to step 2.1.34.
NOTE: The aggregation index (A.I.) calculated from the UV spectra as $OD_{\lambda=350nm}$/ ($OD_{\lambda=280nm}$ - $OD_{\lambda=350nm}$) ×100.[41]

33. Use 100 kDa cutoff centriprep tubes and centrifuge at a velocity of 3,590 x g at 4 °C for a duration of 15 minutes. Collect the liquid that passed through the filter.

34. Dialyze the solution at 4 °C overnight, against Buffer A, using dialysis bags with a 3.5 kDa cutoff.

35. Perform another round of dialysis for a duration of at least 4 hours.

36. Load the dialyzed sample onto a 1 mL MonoQ anion exchange column. Use 30 mM Tris hydrochloride (Tris-HCl) buffer at pH 7.5 as a washing buffer and 30 mM Tris-HCl buffer pH 7.5 with 500 mM NaCl as an elution buffer.

37. Inject the sample to the column. Then wash with 20 column volumes (CVs) of 0% elution buffer and 100% wash buffer in order to remove the unbound proteins.

38. Wash with 7 CVs of 30% elution buffer.

39. Elute the α-Syn protein sample using a gradient that changes from 30% to 100% elution buffer for 30 CVs, at a flow rate of 1.5 mL/min.
NOTE: α-Syn elutes at 46-66 CVs at conductivity 20-24 mS/cm, which is referring to 38-50% elution buffer.

40. Collect the fractions of the main elution peak. Verify the presence of α-Syn by running samples in 15% sodium dodecyl sulfate polyacrylamide gel electrophoresis (SDS-PAGE), following staining with either Coomassie Blue or Fast SeeBand staining solution. A band at 15 kDa is expected.

41. Unify the relevant fractions and dialyze them overnight, against buffer A, using dialysis bags with a 3.5 kDa cutoff at 4 °C.

42. Prepare aliquots of the protein sample and store them at -20 °C.

2. Cy3-labelled α-Synuclein

1. Reduce the thiol of the cysteine residue in the α-Syn A56C mutant by adding DTT to a final concentration of 2 mM for a duration of 1 hour at room temperature.

2. Remove DTT by performing two rounds of dialysis using 3.5 kDa cutoff dialysis bags. For the first round, dialyze against 30 mM Tris-HCl pH 8.0 and 2 mM EDTA. For the second round, dialyze against 50 mM HEPES pH 7.2 and 2 mM EDTA.

3. Reduce the cysteine residues by adding Tris(2-carboxyethyl)phosphine hydrochloride (TCEP) to the protein sample, to a final concentration of 50 µM for a duration of 30 minutes at room temperature.
NOTE: TCEP is a non-sulfhydryl reducing agent, hence it keeps the thiol groups reduced without reacting with the dye. We added 0.5 µL from a stock solution of 1 M TCEP.

4. Calculate the amounts of protein required for the final reaction volume of 1 mL.

   NOTE: Here is an example for the calculation we used:

   $20\ \mu M_{\text{final protein concentration}} \times 1\ mL_{\text{final volume}} = 56\ \mu M_{\text{initial protein concentration}} \times V_{\text{protein to be added}}$

5. Calculate the amount of dye required for final reaction volume of 1 mL. Dye labeling of a single cysteine should be performed with excess dye, at a dye:protein molar ratio of at least 3:1.

   NOTE: An example for the calculation we used:

   $60\ \mu M_{\text{final dye concentration}} \times 1\ mL_{\text{final volume}} = 370\ \mu M_{\text{initial dye concentration}} \times V_{\text{dye to be add}}$

6. Calculate the amount of buffer from the dialysate required to adjust the total reaction volume to 1 mL.

   NOTE: Calculation example: 1 mL - (V calculated from step 2.2.4 + V calculated from step 2.2.5)

7. Prepare reaction vial with a magnet on top of a stirrer.

8. Firstly, add the calculated amount of the protein and the buffer. Afterwards, add the calculated amount of the dye (sulfo-Cy3 maleimide).

9. Keep the reaction at room temperature in the dark for a duration of 3-5 hours.

10. Terminate the reaction by adding 2 mM DTT and continue for a duration of 1 hour.

11. Perform three rounds of dialysis against Buffer A, using dialysis bags with a 3.5 kDa cutoff to remove excess free dye from the solution.

12. Load the sample on a size exclusion column to further separate the labeled α-Syn from the free dye.

13. Determine the concentration of pure labeled α-Syn by measuring the absorption of the dye (absorption coefficient for sulfo-Cy3 is 162,000 M^{-1} cm^{-1} at λ=548 nm).

14. If needed, concentrate the pure labeled α-Syn solution using a vacuum concentrator (e.g., SpeedVac). Then, perform one round of dialysis against buffer A, using dialysis bags with a 3.5 kDa cutoff and again determine the concentration of the labeled protein.

15. Prepare aliquots of the labeled protein sample and store them at -20 °C.

3. Measurements

1. smPIFE experimental setup

   NOTE: Use the following confocal-based setup or similar.

   1. Use a pulsed laser source (in our case, λ= 532 nm picosecond pulsed laser with pulse width of ~100 ps FWHM), operating at a suitable repetition rate (20 MHz in our case) and routed to the SYNC of a time-correlated single photon counting (TCSPC) card, as the source of sulfo-Cy3 (sCy3) excitation.

   2. Use a dichroic mirror with high reflectivity at 532 nm, to separate excitation and scattering from fluorescence.

   3. Use a 100 μm diameter pinhole at the focus of the emitted light, after the collimated emission beam was focused by a lens, and before the emission beam has been re-collimated by another lens.

4. Use a band pass filter (585/40 nm in our case) to further filter sCy3 fluorescence from other light sources.

5. Detect the fluorescence using a detector (single-photon avalanche diode or hybrid photomultiplier, in our case) routed (through a 4-to-1 router, in our case) to a TCSPC module (Becker & Hickl SPC-150, in our case).
   NOTE: In our case, data acquisition is performed via the VistaVision software (ISS^{TM}) in the time-tagged-time-resolved (TTTR) file format.

2. smPIFE sample preparation

   1. Prepare 25 pM sCy3-labeled α-Syn in measurements buffer: 10 mM sodium acetate, 10 mM sodium dihydrogen phosphate, 10 mM glycine pH 8.0, 20 mM NaCl, 10 mM cysteamine and 1 mM 6-hydroxy-2,5,7,8-tetramethylchroman-2-carboxylic acid (TROLOX), in a low protein binding tube.
      NOTE: If α-Syn is measured in the presence of SDS vesicles, add the appropriate SDS amount as well.
   2. Rinse an 18-chamber microscopy coverslip slide with 100 µL of 1 mg/mL bovine serum albumin (BSA) for a duration of 1 minute, and then remove the BSA.
   3. Add 100 µL of the 25 pM sCy3-labeled α-Syn sample to a chamber in the coverslip slide.
   4. Perform smPIFE measurement of the sample using the described setup, as follows in the next steps.

3. smPIFE data acquisition

   1. Use a high numerical aperture water immersion objective lens (in our case, Olympus UPLSAPO 60x N.A. 1.2), and add a drop of ultra-pure water on top of the objective lens.
   2. Fix the coverslip slide in a stage chamber and install it on top of the microscope stage.
   3. Bring the objective lens upwards, until the water droplet on top of the objective lens smears at the bottom of the coverslip slide.
   4. Open the laser shutter and bring the objective lens upwards, while inspecting the pattern on a CMOS camera, collecting light scattered from the sample. Observe the Airy rings pattern: the first one represents the focus at the water-glass interface, and then the second one represents the focus at the interface between the glass and the sample solution.
   5. Increase the height of the objective lens by an additional 75 µm, bringing the laser focus deep into the solution, to minimize auto-fluorescence from the glass surface of the coverslip.
   6. Tune the laser power at the objective lens to be ~100 µW.
   7. Start the acquisition of detected photons for a predefined time (2 hours, in our measurements).
      NOTE: The majority of the acquisition signal should have a rate (measured in counts per seconds, cps) that is similar to that acquired when measuring just the buffer; the millisecond-binned data should show scarce photon burst events, with the majority of bins having an average rate that is comparable to the typical detector background rate (<1,000 cps, in our case).

4. smPIFE burst analysis

1. Raw data conversion

NOTE: The data is usually stored in a binary file with a format that was predefined by the company that manufactures the TCSPC card (.spc files in our case).

1. Convert the raw data file to the photon-HDF5 universal file format[42], using the software suite *phconvert* (https://github.com/Photon-HDF5/phconvert). Call the raw data file as an input and convert into a raw data .hdf5 file using the appropriate code in the *phconvert* suite (the *Convert ns-ALEX Becker-Hickl files to Photon-HDF5.ipynb* Jupyter notebook, in our case).

   NOTE: The conversion into a .hdf5 file includes: (1) determining the relevant photon streams in the raw data (i.e., photon streams of registered photons of the relevant detector ID); (2) the relevant photon nanotimes (the photon detection times relative to the excitation SYNC time); and (3) added metadata.

2. Burst Search and Selection using *FRETbursts*[43]

   NOTE: All of the photon-HDF5 raw data files of the smPIFE measurements, as well as the code summarizing the analysis of the raw data, are stored in Zenodo (https://doi.org/10.5281/zenodo.4587698). All the steps below are detailed and shown within the Jupyter notebooks, also supplied in the Zenodo repository link.

   1. Open the Jupyter Notebooks (within the Anaconda framework, in our case).
   2. Open the notebook *smPIFE-aSyn 56C(Cy3) 25 pM newBuffer (Final notebook).ipynb* (it can be found in the Zenodo link).
   3. Load *FRETbursts*.
   4. Load the photon HDF5 data file.
   5. BG rate assessment: using the histogram of the inter-photon times, calculate the background (BG) rates for each 30 seconds of data acquisition in the photon HDF5 data file.

      NOTE: The following steps describe the burst search using the sliding window algorithm[44,45,46].

   6. Move a time window of m=20 consecutive photons, one photon at a time.
   7. Collect the photon data only if the instantaneous photon rate, $(m/(t_{i+m-1} - t_i))$, is at least F=11 times larger than the BG rate for that period of the data acquisition.

      NOTE: A burst is constructed out of all of the consecutive photons that were collected by sliding the window one photon at a time (step 4.2.6.) and agreeing with the photon rate criterion (step 4.2.7).

   8. Calculate the following burst characteristics:

      Burst size: the amount of photons in a burst.

      Burst duration: the time difference between the last and first photon detection times in a burst.

      Burst brightness: the largest value of the instantaneous photon rate in a burst.

      Burst separation: the time interval between consecutive bursts.

      NOTE: The following points describe the further burst selection procedure.

   9. Plot the histogram of burst brightness values (the highest instantaneous photon rate in a burst), with the events' axis in logarithmic scale.
   10. Define the burst brightness threshold as the minimal burst brightness value from which the histogram exhibits a decaying pattern.

11. Select bursts with brightness values larger than the burst brightness threshold.

    NOTE: The next steps describe burst mean fluorescence lifetimes.

12. Plot the histogram of photon nanotimes for all photons in all selected bursts with the photon counts axis in logarithmic scale.

13. Define the nanotime threshold as the minimal nanotime value from which the histogram of photon nanotimes exhibits a decaying pattern.

14. Select only photons with nanotimes larger than the nanotime threshold.

15. Calculate the algebraic average of all selected photon nanotimes.

16. Subtract the nanotime threshold from the photon nanotime algebraic average. The result is the mean photon nanotime of the burst, which is directly proportional to the mean fluorescence lifetime.

17. Plot the histogram of all burst mean fluorescence lifetimes. Centrally-distributed sub-populations of fluorescence lifetime may appear. Sub-populations with low value averages represent molecule species with sCy3 that was not sterically obstructed, while sub-populations with higher value averages represent molecule species with sCy3 that was more sterically obstructed.

    NOTE: The next steps describe slow between-burst dynamics based on burst recurrence analysis[47]

18. Plot the histogram of burst separation times, with the separation time axis in logarithmic scale.

    NOTE: Two sub-populations of burst separation times will appear:

    A major sub-population with separation times of seconds, representing consecutive bursts originating from different consecutively-measured molecules.

    A minor sub-population with separation times ~<100 ms, representing consecutive bursts both originating from the same molecule, recurring back through the confocal volume.

19. Select to save all pairs of consecutive bursts that are separated by less than a maximal separation time that defines the same-molecule sub-population (<100 ms, in our case).

20. Plot a histogram or a scatter plot of the mean fluorescence lifetimes of the first and second bursts for all pairs of bursts that recurred below a certain separation time threshold

Representative Results

As an IDP, when it is not bound to another biomolecule, α-Syn exhibits structural dynamics between multiple conformations, with transitions at few microseconds[40] and even at hundreds of nanoseconds[41]. When α-Syn crosses the confocal spot, it may undergo thousands of transitions between conformations. Indeed, this was the case when smFRET was used[39,40]. Here we perform smPIFE measurements in order to probe the local conformational dynamics of α-Syn.

The measurement records fluorescence photons emitted from a sulfo-Cy3 (sCy3) dye, attached to the thiol group of cysteine in the α-Syn A56C mutant. The sCy3 fluorophore can undergo isomerization when in excited state. However, sCy3 emits a photon when it de-excites from its *trans* isomer. Therefore, if nothing sterically obstructs the sCy3 excited-state isomerization, it will emit few photons on

average, but will exhibit a low fluorescence quantum yield and short fluorescence lifetime. However, if the excited-state isomerization of sCy3 is obstructed by, for example, the surface of a nearby protein, the rate of isomerization will decrease, which in turn will lead to more de-excitations from the *trans* isomer, and hence more photons, a higher fluorescence quantum yield and longer fluorescence lifetimes. This is better known as the PIFE effect.

Using smPIFE we measured the mean fluorescence lifetime of sCy3 labeling α-Syn at residue 56 one α-Syn at a time, where the sCy3 dye senses the protein environment around residue 56. The protein was measured at a concentration of 25 pM, in which it is mainly found as a monomer. The results of the smPIFE measurements are shown as histograms of mean fluorescence lifetimes of single α-Syn molecules (**Figure 1**). The mean fluorescence lifetimes can be grouped into two major sub-populations (**Figure 1A**). The first sub-population exhibits short fluorescence lifetimes, with a characteristic fluorescence lifetime of 1.6 ns, representing α-Syn conformational states with no or few protein surfaces found in the vicinity of residue 56. The second sub-population exhibits longer fluorescence lifetimes, with a characteristic fluorescence lifetime of 3.5 ns, representing α-Syn conformational states with more protein surfaces found in the vicinity of residue 56.

It is known that in the presence of ~5-10 mM SDS, the N-terminal and NAC segments of almost all of the α-Syn molecules in solution adopt a helical hairpin structure upon binding to SDS vesicles[40]. Since residue 56 is located within the NAC segment, fluorescence from sCy3 labeling residue 56 is expected to sense a rather uniform microenvironment, since the majority of almost all α-Syn molecules should acquire the vesicle-bound helical hairpin structure. Therefore, we performed similar smPIFE measurements but in the presence of 5 mM SDS as a control, expecting to identify a single population of fluorescence lifetimes. Indeed, these measurements result in a single population of fluorescence lifetimes with a characteristic fluorescence lifetime of 3.1 ns (**Figure 1B**). The ~3 ns characteristic fluorescence lifetime points to a local structure in the vicinity of residue 56, that does not exist in the ~1.5 ns lifetime sub-population of α-Syn in solution, emphasizing the structuring α-Syn undergoes when the helical hairpin is formed and the binding to the SDS vesicle surface has occurred. Interestingly, that single population has a shorter characteristic fluorescence lifetime relative to the ~3.5 ns lifetime sub-population of α-Syn in solution.

The appearance of two distinct centrally distributed sub-populations of single-molecule bursts is a well-known signature of molecular heterogeneity. Since no mixture of separate labeled molecules is involved, both lifetime sub-populations represent two separate species of sCy3 labeling residue 56 in α-Syn (**Figure 1A**). Therefore, the results report dynamic heterogeneity. This is because the parameter reported in the histogram is calculated using all the photons in a burst throughout the few ms duration of the diffusing α-Syn inside the confocal volume. Therefore, sCy3-labeled α-Syn molecules crossed the confocal volume either when exhibiting a short or a long mean lifetime. The transitions between these species must occur slower than the characteristic diffusion times through the confocal spot, hence slower than a few milliseconds. In order to assess this dynamic behavior, we performed burst-recurrence analysis[47]. In short, since we seek to assess dynamics that occur at times longer than the duration of a single-molecule burst, we tested the possibility that a single α-Syn molecule exhibits a change in the sCy3 mean fluorescence lifetime between consecutive crossings of the

confocal spot. To do so, we first distinguish between two types of consecutive bursts: i) consecutive bursts of different α-Syn molecules with burst separation times that distribute in seconds, and ii) consecutive bursts of the same α-Syn molecule that recurs in the confocal volume after a burst separation time, at times as slow as ~100 ms (**Figure 2A**). Following the two mean lifetime sub-populations, we chose to inspect pairs of consecutive bursts that are separated by at most 100 ms (**Figure 2A**), where the first out of the pair of bursts exhibited mean fluorescence lifetime within the short lifetime sub-population (0-2 ns) or within the long lifetime sub-population (>3.5 ns; **Figure 2B**, colored shades). The inspection tests which of the bursts of recurring bursts, represented by the second burst in the pair of consecutive bursts, exhibits mean fluorescence lifetime within the lifetime sub-population opposite to the one in the first burst. One can observe that a fraction of molecules that start as a burst in the short lifetime sub-population recur as a burst outside that range and even within the long lifetime subpopulation (**Figure 2C**), and that a fraction of molecules that start as a burst in the long lifetime sub-population recur as a burst outside that range and even within the short lifetime subpopulation (**Figure 2D**), all within 10-100 ms.

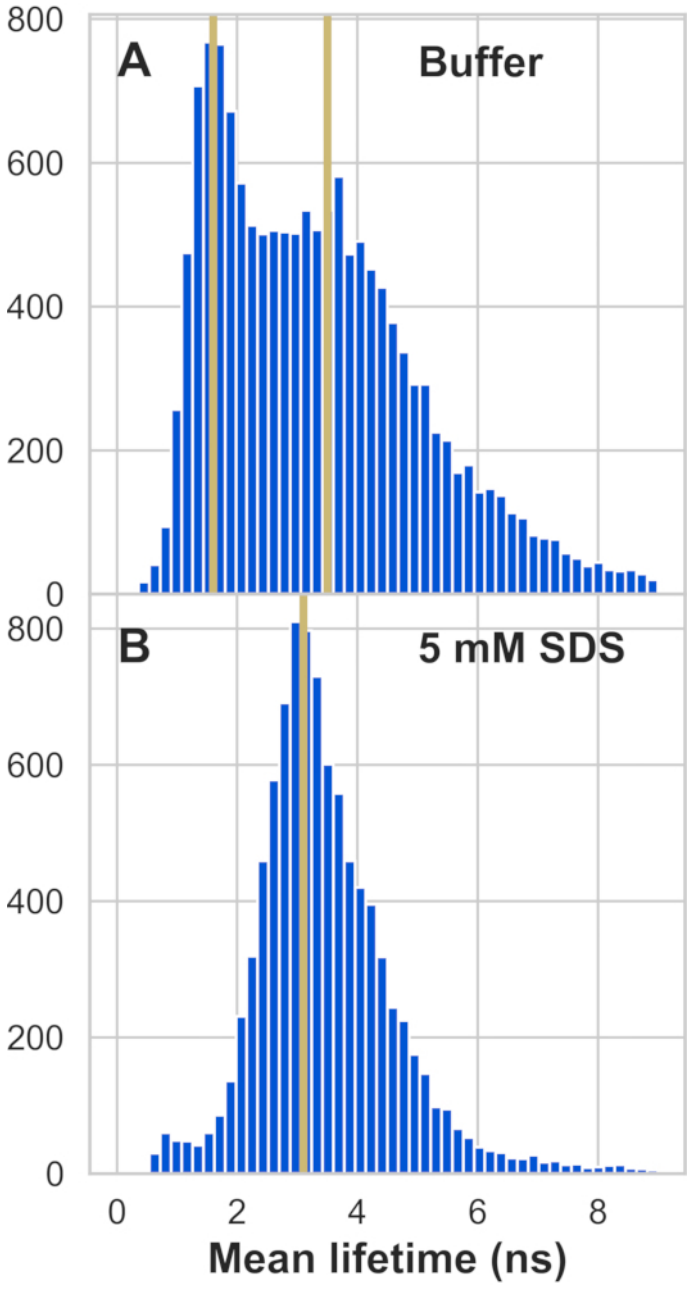

Figure 1: Mean fluorescence lifetime sub-populations of sCy3 labeling residue 56 in α-Syn A56C. mean fluorescence lifetime histograms of freely-diffusing sCy3-labeled α-Syn A56C (at 25 pM) in the absence **(A)** and presence **(B)** of 5 mM SDS. Please click here to view a larger version of this figure.

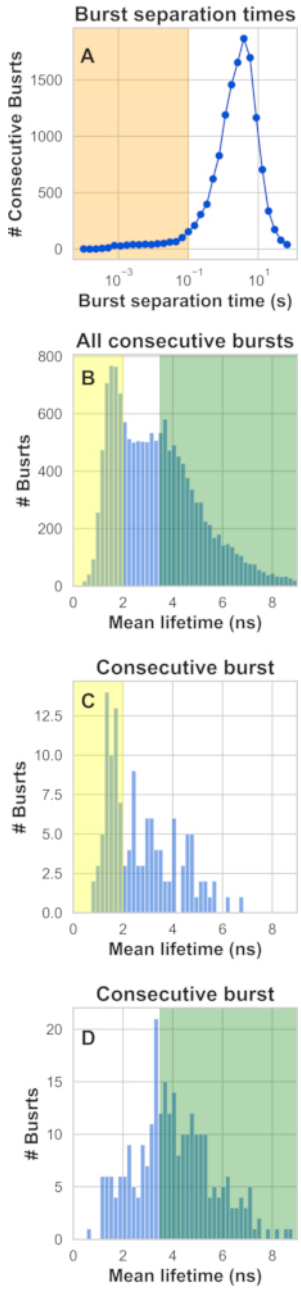

Figure 2: PIFE burst recurrence analysis shows individual molecules undergo transitions between different average lifetime values within 100 ms. From top to bottom: (**A**) the histogram of separation times between consecutive single-molecule bursts. The orange shade represents separation times between consecutive bursts of recurring molecules, where the first and second bursts arise from the same molecule. (**B**) The mean fluorescence lifetime histogram of all single-molecule bursts. The yellow and green shades represent the range of average lifetime values chosen to represent values within short and long mean lifetime sub-populations, respectively. (**C**) or (**D**). The mean fluorescence lifetime histograms of bursts that were separated from a previous burst by a time within the orange-shaded timescale (in **A**), and where the

previous burst had an average lifetime within the range represented by the yellow or green shades, respectively. Please click here to view a larger version of this figure.

Discussion

Extensive biochemical and biophysical studies were performed to study the structural characteristics of α-Syn and its disordered nature[33,34,35,36,37,38]. Several works have already utilized freely-diffusing smFRET to investigate the intra-molecular dynamics of the α-Syn monomer free of binding. These works reported the high dynamic heterogeneity of α-Syn, which leads to averaging-out of multiple different structural species within the typical diffusion times through the confocal spot, leading to the appearance of a single FRET population[39,40]. However, one must remember that smFRET measurements report on changes in inter-dye distances occurring within 3-10 nm, a scale characterizing overall structural changes in a small protein such as α-Syn.

We were curious as to what results we might find when using a different fluorescence-based sensor of spatial changes within a protein that is sensitive to local structural dynamics and that has been utilized also at the single-molecule level. smPIFE can track local spatial changes nearby sCy3 labeling a specific amino acid residue in the 0-3 nm range.

In this study, we utilized smPIFE to investigate the dynamics of local structures within α-Syn and more specifically local structure changes nearby the NAC residue 56. The results suggest that the region in the vicinity of residue 56 in α-Syn exhibits a few distinct structural sub-populations that are stable enough thermodynamically to interconvert in as slow as 100 ms, and perhaps even slower. These sub-populations are identified through the inspection of the mean fluorescence lifetimes of measured sCy3-labeled single α-Syn molecules. In these sub-populations, the longer the characteristic fluorescence lifetime of the sub-population is, the more nearby a protein surface obstructs the excited-state isomerization of sCy3, and hence the closer that protein surface is to that sCy3-labeled residue.

Like other IDPs, α-Syn has been reported to have interactions with other biomolecules, as well as self-association, where in many cases these binding events involve stabilization of a specific structure within the α-Syn subunit[56,57,58,59]. Some proteins acquire a specific structure upon binding, via an induced-fit mechanism. However other proteins spontaneously interconvert between several distinct conformations, and the binding event to a specific biomolecule merely stabilizes one of the preexisting conformations. For the latter case, one of the requirements is that the conformation to be stabilized will survive long enough to accommodate the initial binding. Therefore, the longer a structural region in a protein survives, the higher the binding efficiency will be. We suggest that the observed millisecond-stable sub-populations represent the existence of distinct species of local structure in the vicinity of residue 56. These point to different local structure species nearby the middle of the NAC and NTD segments. In a recent work, we report this and other sCy3-labeled residues in these segments also exhibit such sub-populations[60]. This result comes to show that the structural dynamics of the free α-Syn monomer can be best described as rapid (few microseconds at most[40]) overall protein dynamics, carrying local structural segments that stay stable for milliseconds. Other IDPs such as Tau and amyloid-β were known to share similar characteristics of carrying a local structured region[48,49,50].

smPIFE has been mainly used for studying the interactions between separate biomolecules. Here, we employ smPIFE to investigate PIFE within segments of the same protein. It is important to mention that the majority of previous smPIFE experiments were performed by tracking relative changes in fluorescence intensities of single immobilized sCy3-labeled molecules[13,14,15,16,17,18,19,51,52,53]. While useful for immobilized molecules, this procedure is less informative when measuring freely-diffusing single-molecules. Hwang *et al.* have shown how to measure the PIFE effect also by tracking changes in fluorescence lifetimes, which report directly on the change in the excited-state isomerization dynamics of sCy3[19]. Here we probe the PIFE effect of single diffusing α-Syn via the sCy3 mean fluorescence lifetimes, rather than tracking relative changes in fluorescence intensities. Doing so, we were able to acquire PIFE-related sub-populations despite the short residence time of each single α-Syn molecule in the confocal spot. In fact, the mean fluorescence lifetimes proved to be useful not only in defining PIFE-related sub-populations, but also in assessing slow PIFE-related dynamics using the burst recurrence analysis framework[47]. However, more work is required in developing procedures that will allow to properly assess faster PIFE dynamics. There are plenty of existing photon statistics tools, utilized to assess rapid FRET dynamics in freely diffusing smFRET experiments, which we intend to repurpose to be used in smPIFE[54,55].

To summarize, in this work we used the relatively new combination of PIFE measurements of freely-diffusing single molecules to identify ms-stable sub-populations of local structures in α-Syn, which were not recovered by smFRET. We employed smPIFE measurements to study α-Syn as a model IDP and our results extend beyond past findings of α-Syn being globally disordered. The findings suggest α-Syn may carry ms-stable ordered local structures and we hypothesize these local structures may serve a role in binding recognition.

Thus far, smPIFE was used as means to study interactions of sCy3-labeled nucleic acids with their unlabeled protein counterparts[51]. By that, smPIFE was utilized as a powerful tool to sense biomolecular interactions, and hence the natural next step in that direction would be to use it in order to sense protein-protein interactions and their dynamics, one complex at a time.

The power of using a short-range proximity sensor such as smPIFE can assist in identifying stable local structuring within other protein systems considered disordered and structurally unstable. However, the power of using a single-molecule fluorescence-based short proximity sensor does not stop there. There are many biomolecular systems that exhibit short-scale conformational dynamics to facilitate their function, such as many ion channels. We believe smPIFE can serve as a tool complementary to single-molecule FRET, in such cases where the dynamic range of the proximity changes within the protein system does not match the dynamic range of distances FRET can detect and resolve. In summary, we promote the use of smPIFE as a proximity-sensor complementary to single-molecule FRET measurements, in order to cover a wider scale of biomolecular proximities, and perhaps observe clear millisecond-averaged sub-populations of the measured parameters reporting on stable structures that are either local or overall.

Disclosures

All authors share no conflict of interest.

Acknowledgments

The pT-t7 plasmid encoding A56C α-Syn mutant was given to us as a present from Dr. Asaf Grupi, Dr. Dan Amir and Dr. Elisha Haas. This paper was supported by the National Institutes of Health (NIH, grant R01 GM130942 to E.L. as a subaward), the Israel Science Foundation (grant 3565/20 within the KillCorona - Curbing Coronavirus Research Program), the Milner Fund and the Hebrew University of Jerusalem (startup funds).

References

1. Gust, A. et al. A starting point for fluorescence-based single-molecule measurements in biomolecular research. *Molecules.* **19**, (10) 15824-15865 (2014).
2. Weiss, S. Fluorescence spectroscopy of single biomolecules. *Science.* **283**, (5408) 1676-1683 (1999).
3. Haran, G. Single-molecule fluorescence spectroscopy of biomolecular folding. *Journal of Physics Condensed Matter.* **15**, (32) R1291 (2003).
4. Schuler, B., Lipman, E.A., Eaton, W.A. Probing the free-energy surface for protein folding with single-molecule fluorescence spectroscopy. *Nature.* **419**, (6908) 743-747 (2002).
5. Michalet, X., Weiss, S., Jäger, M. Single-molecule fluorescence studies of protein folding and conformational dynamics. *Chemical Reviews.* **106**, (5)1785-1813 (2006).
6. Ha, T., Enderle, T., Ogletree, D.F., Chemla, D.S., Selvin, P.R., Weiss, S. Probing the interaction between two single molecules: Fluorescence resonance energy transfer between a single donor and a single acceptor. *Proceedings of the National Academy of Sciences of the United States of America.* **93**, (13) 6264-6268 (1996).
7. Deniz, A.A. et al. Single-molecule protein folding: Diffusion fluorescence resonance energy transfer studies of the denaturation of chymotrypsin inhibitor 2. *Proceedings of the National Academy of Sciences of the United States of America.* **97**, (10) 5179-5184 (2000).
8. Bialik, C.N., Wolf, B., Rachofsky, E.L., Ross, J.B.A., Laws, W.R. Dynamics of biomolecules: Assignment of local motions by fluorescence anisotropy decay. *Biophysical Journal*. **75**, (5) 2564–2573 (1998).
9. Jameson, D.M., Sawyer, W.H. Fluorescence anisotropy applied to biomolecular interactions. *Methods in Enzymology.* **246**, 283-300 (1995).
10. Kempe, D., Schöne, A., Fitter, J., Gabba, M. Accurate Fluorescence Quantum Yield Determination by Fluorescence Correlation Spectroscopy. *Journal of Physical Chemistry B.* **119**, (13) 4668-4672 (2015).
11. Callis, P.R., Liu, T. Quantitative Prediction of Fluorescence Quantum Yields for Tryptophan in Proteins. *Journal of Physical Chemistry B.* **108,** 4248-4259 (2004).
12. Lehrer, S.S. Solute Perturbation of Protein Fluorescence. The Quenching of the Tryptophyl Fluorescence of Model Compounds and of Lysozyme by Iodide Ion. *Biochemistry.* **10**, (17) 3254-63 (1971).
13. Xie, K.X., Liu, Q., Jia, S.S., Xiao, X.X. Fluorescence enhancement by hollow plasmonic assembly and its biosensing application. *Analytica Chimica Acta.* **1144**, 96-101 (2021).
14. Stennett, E.M.S., Ciuba, M.A., Lin, S., Levitus, M. Demystifying PIFE: The Photophysics behind the Protein-Induced Fluorescence Enhancement

Phenomenon in Cy3. *Journal of Physical Chemistry Letters.* **6**, (10)1819-1823 (2015).

15. Nguyen, B., Ciuba, M.A., Kozlov, A.G., Levitus, M., Lohman, T.M. Protein Environment and DNA Orientation Affect Protein-Induced Cy3 Fluorescence Enhancement. *Biophysical Journal*. **117**, (1) 66-73 (2019).
16. Song, D., Graham, T.G.W., Loparo, J.J. A general approach to visualize protein binding and DNA conformation without protein labelling. *Nature Communications.* **7**, 10976 (2016).
17. Ploetz, E. et al. Förster resonance energy transfer and protein-induced fluorescence enhancement as synergetic multi-scale molecular rulers. *Scientific Reports.* **6**, 33257 (2016).
18. Hwang, H., Myong, S. Protein induced fluorescence enhancement (PIFE) for probing protein-nucleic acid interactions. *Chemical Society Reviews.* **43**, (4) 1221-1229 (2014).
19. Hwang, H., Kim, H., Myong, S. Protein induced fluorescence enhancement as a single molecule assay with short distance sensitivity. *Proceedings of the National Academy of Sciences of the United States of America.* **108**, (18) 7414-7418 (2011).
20. Ray, P.C., Fan, Z., Crouch, R.A., Sinha, S.S., Pramanik, A. Nanoscopic optical rulers beyond the FRET distance limit: Fundamentals and applications. *Chemical Society Reviews.* **43**, 6370-6404 (2014).
21. Chen, H., Rhoades, E. Fluorescence characterization of denatured proteins. *Current Opinion in Structural Biology.* **18**, (4) 516-524 (2008).
22. Alderson, T.R., Markley, J.L. Biophysical characterization of α-synuclein and its controversial structure. *Intrinsically Disordered Proteins.* **1**, (1)18-39 (2013).
23. Mane, J.Y., Stepanova, M. Understanding the dynamics of monomeric, dimeric, and tetrameric α-synuclein structures in water. *FEBS Open Bio.* **6**, (7) 666-686 (2016).
24. Wang, W. et al. A soluble α-synuclein construct forms a dynamic tetramer. *Proceedings of the National Academy of Sciences of the United States of America.* **108**, (43) 17797-17802 (2011).
25. Bartels, T., Choi, J.G., Selkoe, D.J. α-Synuclein occurs physiologically as a helically folded tetramer that resists aggregation. *Nature.* **477**, (7362) 107-110 (2011).
26. Ulmer, T.S., Bax, A., Cole, N.B., Nussbaum, R.L. Structure and dynamics of micelle-bound human α-synuclein. *Journal of Biological Chemistry.* **280**, (10) 9595-9603 (2005).
27. Georgieva, E.R., Ramlall, T.F., Borbat, P.P., Freed, J.H., Eliezer, D. Membrane-bound α-synuclein forms an extended helix: Long-distance pulsed ESR measurements using vesicles, bicelles, and rodlike micelles. *Journal of the American Chemical Society.* **130**, (39) 12856-12857 (2008).
28. Trexler, A.J., Rhoades, E. α-Synuclein binds large unilamellar vesicles as an extended helix. *Biochemistry.* **48**, (11) 2304–2306 (2009).
29. Stephens, A.D., Zacharopoulou, M., Kaminski Schierle, G.S. The Cellular Environment Affects Monomeric α-Synuclein Structure. *Trends in Biochemical Sciences.* **44**, (5) 453-466 (2019).
30. Illes-Toth, E., Dalton, C.F., Smith, D.P. Binding of dopamine to alpha-synuclein is mediated by specific

conformational states. *Journal of the American Society for Mass Spectrometry*. **24**, (9)1346-1354 (2013).

31. Frimpong, A.K., Abzalimov, R.R., Uversky, V.N., Kaltashov, I.A. Characterizationof intrinsically disordered proteins with electrospray inization mass spectrometry: Conformationl heterogeneity of α-synuciein. *Proteins: Structure, Function and Bioinformatics.* **78**, (3) 714–722 (2010).
32. Sandal, M. et al. Conformational equilibria in monomeric α-synuclein at the single-molecule level. *PLoS Biology.* **6**, (1) e6 (2008).
33. Brodie, N.I., Popov, K.I., Petrotchenko, E. V., Dokholyan, N. V., Borchers, C.H. Conformational ensemble of native α-synuclein in solution as determined by short-distance crosslinking constraint-guided discrete molecular dynamics simulations. *PLoS Computational Biology.* **15**, (3) e1006859 (2019).
34. Ullman, O., Fisher, C.K., Stultz, C.M. Explaining the structural plasticity of α-synuclein. *Journal of the American Chemical Society.* **133**, (48) 19536-19546 (2011).
35. Binolfi, A., Theillet, F.X., Selenko, P. Bacterial in-cell NMR of human α-synuclein: A disordered monomer by nature? *Biochemical Society Transactions.* **40**, (5) 950-954 (2012).
36. Waudby, C.A. et al. In-Cell NMR Characterization of the Secondary Structure Populations of a Disordered Conformation of α-Synuclein within E. coli Cells. *PLoS ONE.* **8**, (8) e72286 (2013).
37. Yu, J., Malkova, S., Lyubchenko, Y.L. α-Synuclein Misfolding: Single Molecule AFM Force Spectroscopy Study. *Journal of Molecular Biology.* **384**, (4) 992-1001 (2008).
38. Guerrero-Ferreira, R., Kovacik, L., Ni, D., Stahlberg, H. New insights on the structure of alpha-synuclein fibrils using cryo-electron microscopy. *Current Opinion in Neurobiology.* **61**, 89-95 (2020).
39. Trexler, A.J., Rhoades, E. Single molecule characterization of α-synuclein in aggregation-prone states. *Biophysical Journal.* **99**, (9) 3048-55 (2010).
40. Ferreon, A.C.M., Gambin, Y., Lemke, E.A., Deniz, A.A. Interplay of α-synuclein binding and conformational switching probed by single-molecule fluorescence. *Proceedings of the National Academy of Sciences of the United States of America.* **106**, (14) 5645-5650 (2009).
41. Rezaei-Ghaleh, N. et al. Local and Global Dynamics in Intrinsically Disordered Synuclein. *Angewandte Chemie - International Edition.* **57**, (46) 15262-15266 (2018).
42. Ingargiola, A., Laurence, T., Boutelle, R., Weiss, S., Michalet, X. Photon-HDF5: An Open File Format for Timestamp-Based Single-Molecule Fluorescence Experiments. *Biophysical Journal*. **110**, (1) 26-33 (2016).
43. Ingargiola, A., Lerner, E., Chung, S.Y., Weiss, S., Michalet, X. FRETBursts: An open source toolkit for analysis of freely-diffusing Single-molecule FRET. *PLoS ONE*. **11**, (8) e0160716 (2016).
44. Ingargiola, A. et al. Multispot single-molecule FRET: Highthroughput analysis of freely diffusing molecules. *PLoS ONE.* **12**, (4) e0175766 (2017).
45. Eggeling, C., Fries, J.R., Brand, L., Günther, R., Seidel, C.A.M. Monitoring conformational dynamics of a single molecule by selective fluorescence spectroscopy. *Proceedings of the National Academy of Sciences of the United States of America.* **95**, (4) 1556-1561 (1998).

46. Fries, J.R., Brand, L., Eggeling, C., Köllner, M., Seidel, C.A.M. Quantitative identification of different single molecules by selective time-resolved confocal fluorescence spectroscopy. *Journal of Physical Chemistry A.* **102**, 6601-6613 (1998).

47. Hoffmann, A. et al. Quantifying heterogeneity and conformational dynamics from single molecule FRET of diffusing molecules: Recurrence analysis of single particles (RASP). *Physical Chemistry Chemical Physics.* **13**, (5) 1857-1871 (2011).

48. Eakin, C.M., Berman, A.J., Miranker, A.D. A native to amyloidogenic transition regulated by a backbone trigger. *Nature Structural and Molecular Biology.* **13**, (3) 202-208 (2006).

49. Jahn, T.R., Parker, M.J., Homans, S.W., Radford, S.E. Amyloid formation under physiological conditions proceeds via a native-like folding intermediate. *Nature Structural and Molecular Biology.* **13**, (3) 195-201 (2006).

50. Chen, D. et al. Tau local structure shields an amyloid-forming motif and controls aggregation propensity. *Nature Communications*. **10**, (1) 2493 (2019).

51. Lerner, E., Ploetz, E., Hohlbein, J., Cordes, T., Weiss, S. A Quantitative Theoretical Framework for Protein-Induced Fluorescence Enhancement-Förster-Type Resonance Energy Transfer (PIFE-FRET). *Journal of Physical Chemistry. B.* **120**, (26) 6401-6410 (2016).

52. Valuchova, S., Fulnecek, J., Petrov, A.P., Tripsianes, K., Riha, K. A rapid method for detecting protein-nucleic acid interactions by protein induced fluorescence enhancement. *Scientific Reports*. **6**, 39653 (2016).

53. Qiu, Y., Myong, S. Single-Molecule Imaging With One Color Fluorescence. *Methods in Enzymology.* **581**, 33-51 (2016).

54. Lerner, E. et al. Toward dynamic structural biology: Two decades of single-molecule Förster resonance energy transfer. *Science.* **359**, (6373) eaan1133 (2018).

55. Lerner, E. et al. FRET-based dynamic structural biology: Challenges, perspectives and an appeal for open-science practices. *Elife.* **10**, e60416 (2021).

56. Wang, W. et al. A soluble α-synuclein construct forms a dynamic tetramer. *Proceedings of the National Academy of Sciences of the United States of America.* **108**, (43)17797-17802 (2011).

57. Bartels, T., Choi, J.G., Selkoe, D.J. α-Synuclein occurs physiologically as a helically folded tetramer that resists aggregation. *Nature.* **477**, (7362) 107-110 (2011).

58. Ulmer, T.S., Bax, A., Cole, N.B., Nussbaum, R.L. Structure and dynamics of micelle-bound human α-synuclein. *Journal of Biological Chemistry.* **280**, (10) 9595-9603 (2005).

59. Georgieva, E.R., Ramlall, T.F., Borbat, P.P., Freed, J.H., Eliezer, D. Membrane-bound α-synuclein forms an extended helix: Long-distance pulsed ESR measurements using vesicles, bicelles, and rodlike micelles. *Journal of the American Chemical Society.* **130**, (39) 12856-12857 (2008).

60. Chen, J. et al. The structural heterogeneity of α-synuclein is governed by several distinct subpopulations with interconversion times slower than milliseconds. *Structure.* **29**, (9) (2021).